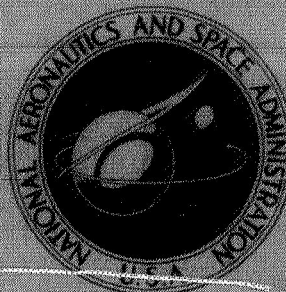


N71-23932

**NASA TECHNICAL
MEMORANDUM**



NASA TM X-2277

NASA TM X-2277

**CASE FILE
COPY**

**RESULTS OBTAINED IN NASA LEWIS
CLOSED-CYCLE MAGNETOHYDRODYNAMIC
POWER GENERATION EXPERIMENTS**

by Ronald J. Sovie and Lester D. Nichols

*Lewis Research Center
Cleveland, Ohio 44135*

1. Report No. NASA TM X-2277	2. Government Accession No.	3. Recipient's Catalog No.	
4. Title and Subtitle RESULTS OBTAINED IN NASA LEWIS CLOSED-CYCLE MAGNETOHYDRODYNAMIC POWER GENERATION EXPERIMENTS		5. Report Date April 1971	
		6. Performing Organization Code	
7. Author(s) Ronald J. Sovie and Lester D. Nichols		8. Performing Organization Report No. E-6158	
		10. Work Unit No. 129-02	
9. Performing Organization Name and Address Lewis Research Center National Aeronautics and Space Administration Cleveland, Ohio 44135		11. Contract or Grant No.	
		13. Type of Report and Period Covered Technical Memorandum	
12. Sponsoring Agency Name and Address National Aeronautics and Space Administration Washington, D.C. 20546		14. Sponsoring Agency Code	
15. Supplementary Notes			
16. Abstract <p>Experiments were performed over a wide range of operating conditions with two magnetohydrodynamic channels. Both channels contained 28 pairs of thoriated tungsten electrodes. In the first channel (length, 195 cm; height, 19 cm; and width, 6.35 cm) open-circuit voltages up to 70 V (0.75 theoretical) were obtained. However, short-circuit currents were limited to 100 to 200 mA at equilibrium conditions and to 100 to 800 mA when preionizers and starter circuits were used. The experimentally determined apparent Hall parameter varied from 0.1 to 0.5 for these conditions. The data indicated that large voltage drops near the electrode surfaces were limiting the short-circuit currents. The second channel was used in an attempt to increase the open-circuit voltage and overcome these losses. In this channel, the width was reduced to 3.8 cm in the electrode region. The effects of internal wall and boundary-layer current leakage were accentuated in this channel, however, and the open-circuit voltage was decreased. Short-circuit currents near the expected equilibrium values were obtained at values of the Hall parameter of about 1. These currents decreased sharply as the magnetic field was increased.</p>			
17. Key Words (Suggested by Author(s)) Plasma physics MHD (magnetohydrodynamics)		18. Distribution Statement Unclassified - unlimited	
19. Security Classif. (of this report) Unclassified	20. Security Classif. (of this page) Unclassified	21. No. of Pages 17	22. Price* \$3.00

RESULTS OBTAINED IN NASA LEWIS CLOSED-CYCLE MAGNETOHYDRO- DYNAMIC POWER GENERATION EXPERIMENTS

by Ronald J. Sovie and Lester D. Nichols

SUMMARY

Experiments were performed over a wide range of operating conditions with two magnetohydrodynamic channels. Both channels contained 28 pairs of thoriated tungsten electrodes. In the first channel (length 195 cm; height 19 cm; and with 6.35 cm) open-circuit voltages up to 70 V (0.75 theoretical) were obtained. However, short-circuit currents were limited to 100 to 200 mA at equilibrium conditions and to 100 to 800 mA when preionizers and starter circuits were used. The experimentally determined apparent Hall parameter varied from 0.1 to 0.5 for these conditions. The data indicated that large voltage drops near the electrode surfaces were limiting the short-circuit currents. The second channel was used in an attempt to increase the open-circuit voltage and overcome these losses. In this channel, the width was reduced to 3.8 cm in the electrode region. The effects of internal wall and boundary-layer current leakage were accentuated in this channel, however, and the open-circuit voltage was decreased. Short-circuit currents near the expected equilibrium values were obtained at values of the Hall parameter of about 1. These currents decreased sharply as the magnetic field was increased.

INTRODUCTION

The purpose of the experimental magnetohydrodynamic (MHD) program at Lewis is to evaluate the feasibility of generating MHD power for space with an input gas temperature of about 2000 K through the use of nonequilibrium ionization. The critical question in this concept is whether the current flowing in the generator will heat the electrons above the equilibrium gas temperature and thereby increase the degree of ionization and gas conductivity sufficiently to make this mode of power generation efficient.

The NASA Lewis closed-loop facility operates at an input temperature of 2000 to 2100 K with an argon-cesium working fluid. With the exception of the cesium seed sys-

tem the loop is operated continuously at these temperatures. Two series of experiments have been completed to date in this facility. The results of the first five tests, in which the general design and structural integrity of the facility were studied, were reported in 1968 (ref. 1). These tests primarily studied the problems involved in sustaining stagnation temperatures of 2100 K for extended periods of time.

In the second series of tests the facility was run many times at stagnation temperatures of 2000 to 2100 K and an entrance Mach number of 0.38 to 0.41. The primary objective of these tests was to obtain the proper working fluid conditions in the generator region. Preliminary results were reported in 1970 (ref. 2). The generator results for these tests were characterized by reasonable open-circuit voltages (70 to 75 percent of theoretical) and very low short-circuit currents (10 percent of theoretical equilibrium values). In an effort to improve these results, the facility has been modified by the addition of an impurity purge system, a new cesium vaporizer, a new preionization system, and various starter circuits. The heater end bell was also redesigned to eliminate a source of electrode coatings. The results of tests run with these modifications and in test sections of different widths are discussed in this report.

SYMBOLS

A	area, m^2
B	magnetic-field strength, T
h	channel height, cm
I_{sc}	short-circuit current, A
l	length, cm
M	Mach number
\dot{m}_A	argon mass flow, kg/sec
p	pressure, N/m^2
S	cesium seed fraction
T_g	gas temperature, K
u	gas velocity, m/sec
V_H	Hall voltage, V
V_{H6-9}	Hall voltage for electrode pair 6-9, V
V_{oc}	Faraday open circuit-voltage, V

w	channel width, cm
β_{app}	apparent Hall parameter, $V_H h / V_{oc} l$
η_R	reheater efficiency, percent
η_H	heater efficiency, percent
σ	plasma conductivity, mho/m

FACILITY

General Description

Figure 1 is a schematic of the closed-loop facility and figure 2 is a cutaway drawing of the high-temperature components located in the test cell. A detailed description of the various system components is given in reference 1. The gas leaving the compressor is preheated in a parallel-flow regenerative heat exchanger (preheater) before entering the graphite resistance heater. On leaving the heater through the nozzle the hot gas enters the MHD channel, expands in the diffuser, and enters the shell side of the reheater. From this point conventional equipment cools, dries, and filters the gas as it flows toward the compressor. The flow-control valve loads the compressor. The bypass valve permits a wide variation of mass flow through the heater. Typical gas temperatures at various points in the loop and the efficiencies of various loop components are indicated in figure 1.

Magnetohydrodynamic Channels

Experiments were performed using two constant-area channel geometries. The dimensions of channel 1 were length l , 195 cm; height h , 19 cm; and width w , 6.35 cm. For channel 2 the width was reduced to 3.8 cm in the electrode region. Figure 3 is a photograph of channel 1 with one side removed and shows the location of the various electrodes and the cesium injection tube. The electrode region of both channels contains 28 pairs of thoriated tungsten electrodes on 2.54-cm centers located in the middle third of the channel. The electrodes are positioned in the center of a 91.4 cm magnetic-field region. Preionization power is added in the magnetic-field direction through seven pairs of electrodes located in the channel sidewalls between the anode and cathode of Faraday electrode pair 1. These electrodes are also used as voltage probes in equilibrium runs. A similar pair of sidewall electrodes is used to heat the cathode of

Faraday electrode pair 26. The cesium vapor is added to the gas stream through an injection tube located in the center of the channel 46 cm upstream of the first electrode pair. Finally, it should be noted that the electrodes protrude 0.6 cm into the gas stream.

Cesium Injection System

In the present tests the liquid cesium was fed to an electrically heated Inconel spiral and was vaporized, and the vapor was injected uniformly along the channel height through a series of holes in a molybdenum injection tube. In channel 1 the hole diameters were 0.75 mm, and the cesium was injected in the direction of the gas flow. In channel 2 the hole diameters were reduced to 0.35 mm, and the cesium was injected in the upstream direction. In both cases a load cell arrangement monitored the weight flow of cesium of the cesium reservoir. These data are recorded on a strip chart that simultaneously records the generator Faraday voltage.

EXPERIMENTAL PROCEDURE

The gas stagnation temperature and high-temperature loop components are slowly brought up to the desired temperature over a period of about 20 hr. The final adjustments of the argon mass flow and entrance Mach number are then made. The loop is then baked out at the operating temperature (2000 to 2100 K) until the minimum impurity level is obtained. The cesium injection runs are then made. In these runs the desired magnetic-field strength, load bank conditions, preionizer and starter circuits, etc., are set, and the cesium is injected for periods varying from 6 to 30 sec. During the injection time all gas properties, vaporizer temperatures, magnetic-field changes, applied power supplies, and electrode data are monitored. The Faraday voltages and currents are monitored for each electrode pair. The Hall voltage V_H is monitored between arbitrarily selected electrodes (e.g., between electrode pairs 6 and 9, V_{H6-9}) rather than between adjacent electrodes.

Prior to some cesium runs, external power supplies are used to run discharges from one electrode pair to another (cathode 1 to cathode 2, etc.). This discharge heats the electrodes and appears to reduce the effects of coatings which sometimes form on the electrode surfaces. In other runs such a discharge is used as a virtual cathode and makes it possible to determine the effects of electrode resistance on the data. Finally, capacitor starter circuits may also be used. These circuits consist of a capacitor and

diode in parallel. The full capacitor voltage (300 V) is applied across the load circuit contactor of an electrode pair to initiate the current flow.

RESULTS FOR CHANNEL 1

The operating conditions for the constant-area channel were gas stagnation temperature T_g , 2030 to 2100 K; stagnation pressure p , 2.3×10^5 N/m²; argon mass flow rate \dot{m}_A , 1.6 to 1.7 kg/sec; gas velocity u , 280 to 300 m/sec; cesium seed fraction S , 0.06 = 0.2 percent; impurity levels, 0.13 percent hydrogen and 0.05 to 0.15 percent carbon monoxide; and magnetic-field strength B , 0.6 to 1.8 T. The Mach number M at the channel entrance was 0.345, and the theoretical open-circuit voltage uBh , was 53.5 V at $B = 1$ T.

The ratio of the measured open-circuit voltage V_{oc} to the theoretical value uBh is plotted against magnetic-field strength in figure 4. The figure shows that this ratio is not a very strong function of B . It varies from roughly 0.8 at $B = 0.6$ T to 0.64 at $B = 1.8$ T. A typical variation of V_{oc} along the channel length is shown in figure 5. The figure shows that the voltage is fairly uniform along the channel and that there are no severe end effects. The voltage at electrode pair 1 is somewhat lower than at the others. This fact is noted here since the vertical voltage profile measurements to be discussed are made at this electrode pair.

The short-circuit current I_{sc} did vary somewhat along the channel and also changed after the starter circuits were used. A typical variation of I_{sc} along the channel is presented in figure 6 for $B = 1.44$ T and no preionization power. Applying preionization power made little difference in the I_{sc} values before any starter circuits were used. The results were somewhat different, however, after the capacitor starter and external power supplies had been used on the electrodes. Consider the data for electrode pairs 1 to 10 shown in figure 7. The figure shows that the currents are increased when preionization power is applied and further increased when the capacitor starter sequence is used. In the latter case (run C) the electrodes are initially open circuited. After the cesium flow is established, the capacitor starter is used to initiate current flow in electrode pair 1. The remaining electrode pairs are then short circuited in sequence. Currents in the range 700 to 900 mA have also been obtained in similar tests and in tests made using the virtual cathode. From the measured V_{oc} and V_H the minimum apparent Hall parameter β_{app} may be calculated by using the relation $\beta_{app} = V_H h / V_{oc} l$. For runs A, B, and C in figure 7 β_{app} increased from 0.09 to 0.33 to 0.53, respectively. The theoretical β for these runs is about 12. For this channel the Hall fields at open-circuit conditions are about 5 V/m, and Hall fields up to 150 V/m are attained at short-circuit conditions.

The voltage profile measurements made at electrode pair 1 at equilibrium conditions and $B = 1.46 \text{ T}$ are shown in figure 8. The theoretical u_{Bh} is also shown for comparison. Comparing the slope of the theoretical u_{Bh} with the voltages measured between probes, one sees that nearly the full theoretical voltage is obtained in the region between probe A and the cathode. The voltage generated between probes also varies somewhat. These data indicate that the internal leakage effects may vary along the height of the channel. The fact that the short-circuit profile is close to the open-circuit data in the region between probes C and G indicates that there is little change in current for these two cases. There are large voltage drops between the outer probes and the electrodes at short-circuit conditions.

In summary, then, reasonable open-circuit voltages were obtained in channel 1. The various starting procedures permit the short-circuit current to be increased from about 100 to 200 mA to values as high as 900 mA. The use of such procedures did not eliminate any major loss mechanism, however, since the theoretical equilibrium current for these conditions is about 10 A. The voltage profile measurements showed large voltage drops at the electrodes. An inspection of the electrodes after the runs showed none of the severe coatings reported previously (ref. 2). However, there was a thin film on some electrode surfaces that had a high resistance at room temperature. Applying power supplies across the Faraday electrodes during the run had shown that, once the current flow was initiated, currents of the order of amperes could be maintained at voltages of 100 to 120 V. It was therefore decided to attempt to increase the generator voltage at the same B by increasing the gas velocity. This was accomplished by decreasing the channel area in the electrode region.

RESULTS IN CHANNEL 2

Channel 2 was identical to channel 1 with the exception that the width was reduced to 3.8 cm in the electrode region. The cesium injection system was also changed slightly. The holes in the injection tube were reduced in diameter from 0.75 to 0.35 mm, and the cesium was injected in the upstream direction to promote better mixing. Higher cesium seed rates were also used to ensure cesium coverage of the electrode surfaces and also to reduce the theoretical value of β . The injection system worked reasonably well, and traces of the open-circuit voltage and short-circuit current during the cesium injection time are shown in figure 9.

The operating conditions for the tests with channel 2 were T_g , 1960 K; p , $2.3 \times 10^5 \text{ N/m}^2$; \dot{m}_A , 1.54 kg/sec; S , 0.2 to 0.6 percent; impurity levels, 0.1 percent and 0.1 percent carbon monoxide, and B , 0 to 1.8 T. At the channel entrance M was

0.31, and u was 256 m/sec. In the smaller area electrode region u was 480 m/sec and T_g was 1830 K at electrode pair 1.

The variation of V_{oc}/uBh with B is compared with the data from channel 1 in figure 10. The magnitudes of the open-circuit voltages obtained were lower in the second channel. It appears that the smaller area of channel 2 makes it more susceptible to wall and boundary-layer leakage effects than channel 1. The variation of V_{oc} along the channel length is shown in figure 11. The ideal value uBh divided by 2 is also shown for comparison. The voltage falls considerably in the exit region. The tests in this channel were made over a wide range of operating conditions. Typical variations of V_{oc} , V_H , and I_{sc} as functions of magnetic field for $S = 0.5$ percent are shown in figure 12. These results are for electrodes near the front of the electrode region that are not affected by the exit end effects. The figure shows that for B above 0.35 T the current decreases with B and that the open-circuit voltage is not a very strong function of B .

All the tests in channel 2 were run without preionization. However, the currents obtained again increased after the various starter circuits had been used. This fact is illustrated by the data presented in figure 13. In this figure the ratios of the measured I_{sc} , V_{oc} , and V_H to the ideal quantities $ouBA_y$, uBh , and βuBl are plotted against the theoretical value of the Hall parameter β . All the ratios decrease with increasing β . The I_{sc} value after the starter circuits were used is near the equilibrium value at low β but decreases sharply with increasing β . This indicates that there is severe internal shorting in the Hall direction. Voltage profile results in channel 2 are shown in figure 14. The open-circuit voltage data show that most of the voltage measured between the cathode and anode is generated in the regions from probe B to the cathode and from the anode to probe G. The region between probes A and G is essentially short circuited. This is further illustrated by the short-circuit data which show that the profile between A and G is about identical to the open-circuit results. Therefore, it appears that at least the interior part of the generator is shorted in both the Hall and Faraday directions.

CONCLUDING REMARKS

The results obtained in these tests have indicated that the currents generated are limited by electrode losses and internal shorting in the Hall direction. The electrode losses can be reduced by the use of the various starting techniques employed in the tests. The internal shorting appears to be along the channel sidewalls and is most severe in the narrow channel. At present the channel geometry is being changed back to the channel 1 design. Probes are being added such that Faraday and Hall potential profiles can be

obtained at various axial and vertical positions along the channel. Probes to measure the vertical and horizontal velocity profiles are also being incorporated in the channel. The Faraday electrodes are also being brought flush with the walls. These changes should better establish the causes and location of the current leakages and perhaps lead to methods of reducing them.

Lewis Research Center,
National Aeronautics and Space Administration,
Cleveland, Ohio, February 22, 1971,
129-02.

REFERENCES

1. Nichols, Lester D.; Morgan, James L.; Nagy, Lawrence A.; Lamberti, Joseph M.; and Ellson, Robert A.: Design and Preliminary Operation of the Lewis Magnetohydrodynamic Generator Facility. NASA TN D-4867, 1968.
2. Sovie, R. J.; and Nichols, L. D.: Results of Initial Subsonic Tests in the NASA-Lewis Closed Loop MHD Generator. Proceedings of the Eleventh Symposium on the Engineering Aspects of Magnetohydrodynamics. D. G. Elliott, ed., Mississippi Univ. Press, 1970, pp. 82-89.

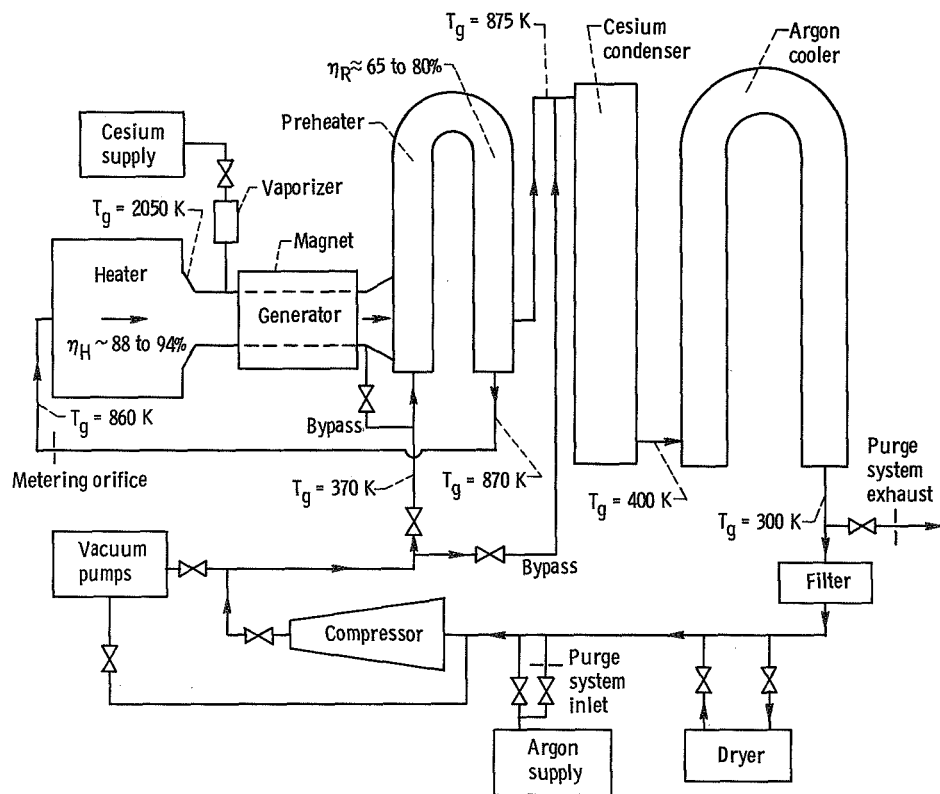


Figure 1. - Loop schematic.

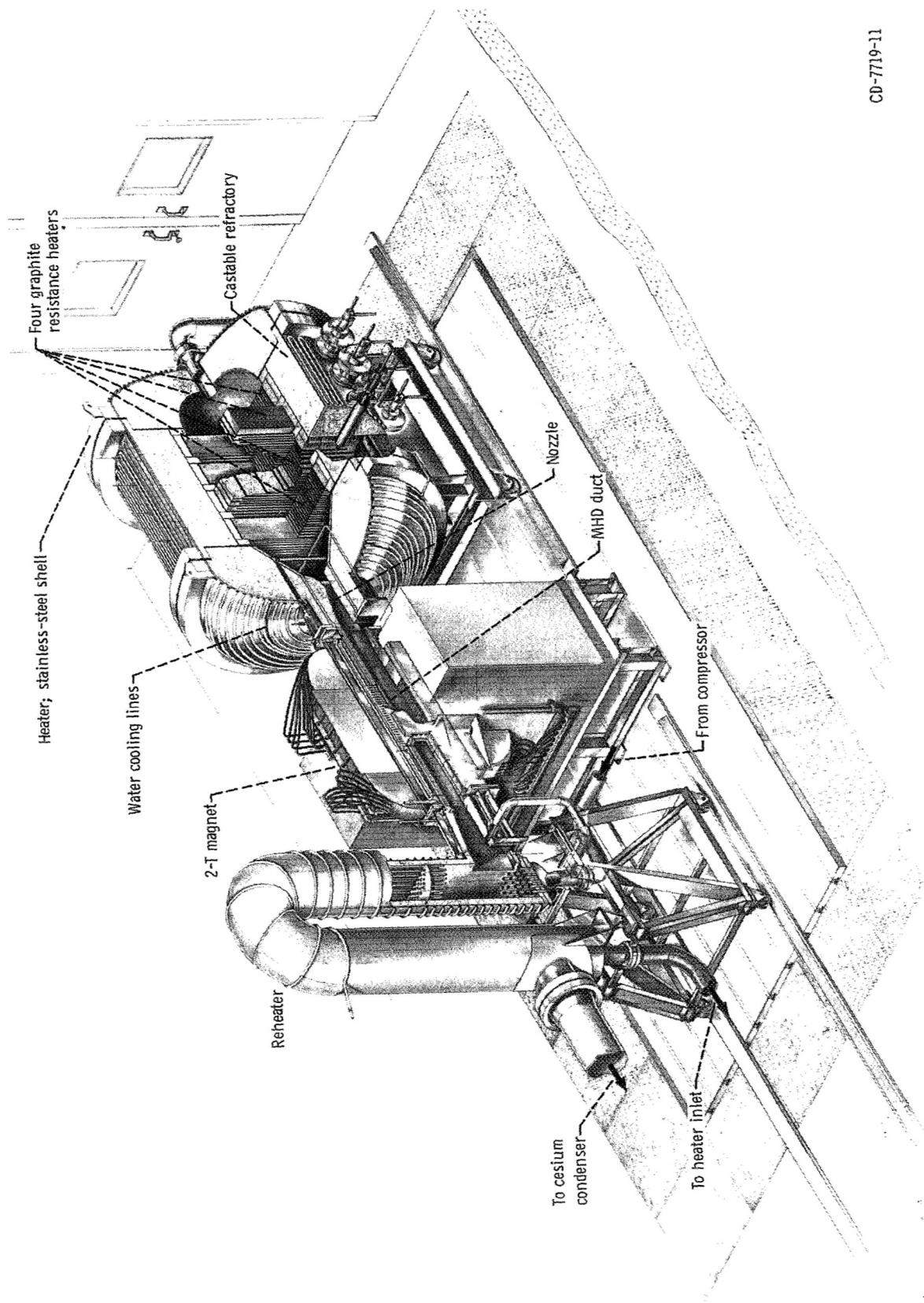


Figure 2. - Bedplate showing heater, nozzle MHD duct, magnet, and reheater. The flow distributor at the heater inlet is not shown.

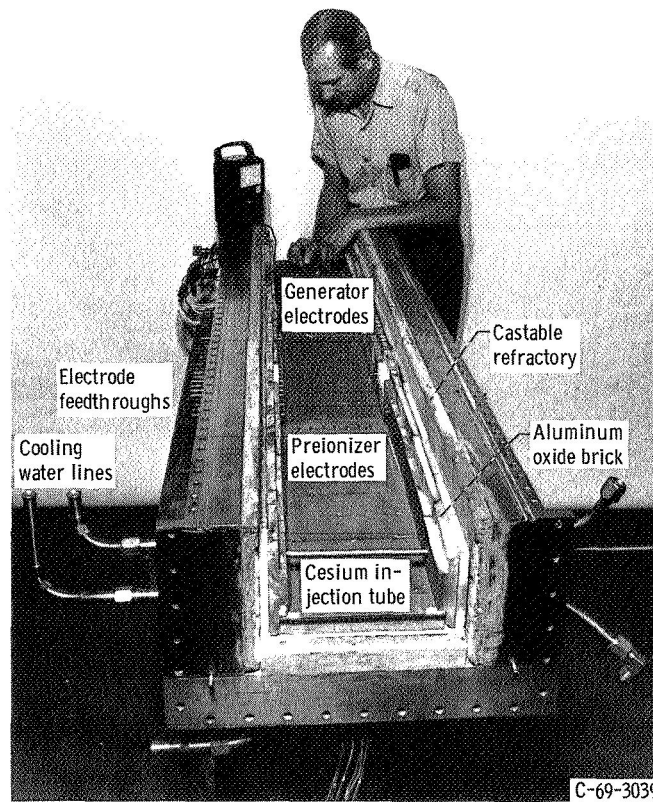


Figure 3. - MHD channel 1.

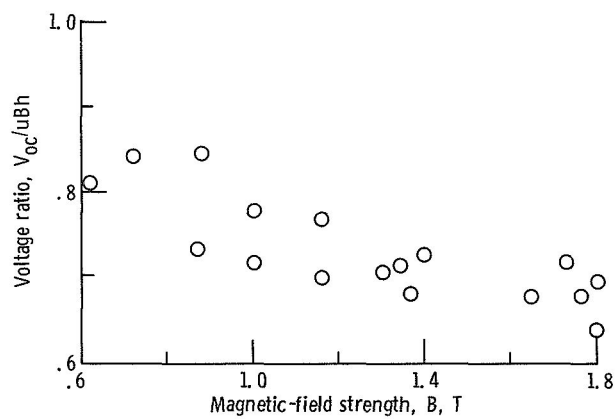


Figure 4. - Ratio of measured open-circuit voltage to theoretical value as function of magnetic-field strength for constant-area channel.

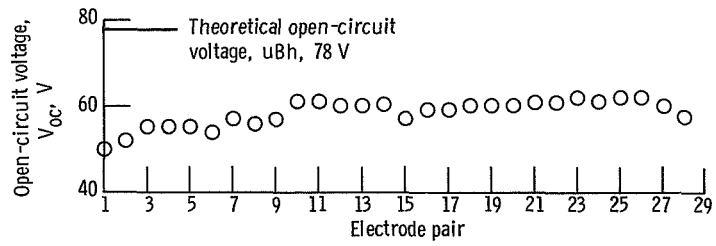


Figure 5. - Variation of open-circuit voltage along channel. Magnetic-field strength, 1.46 T.

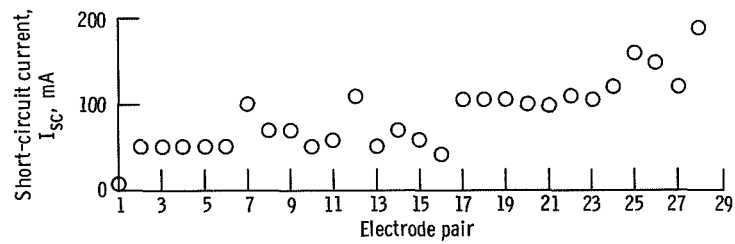


Figure 6. - Variation of short-circuit current along channel length. Magnetic-field strength, 1.44 T.

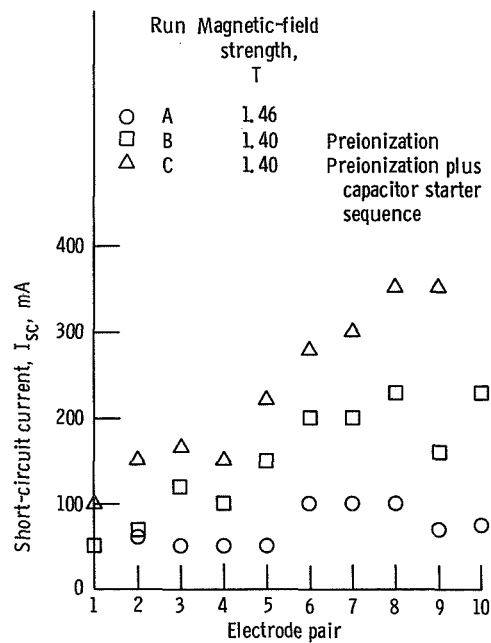


Figure 7. - Variation of short-circuit with operating condition.

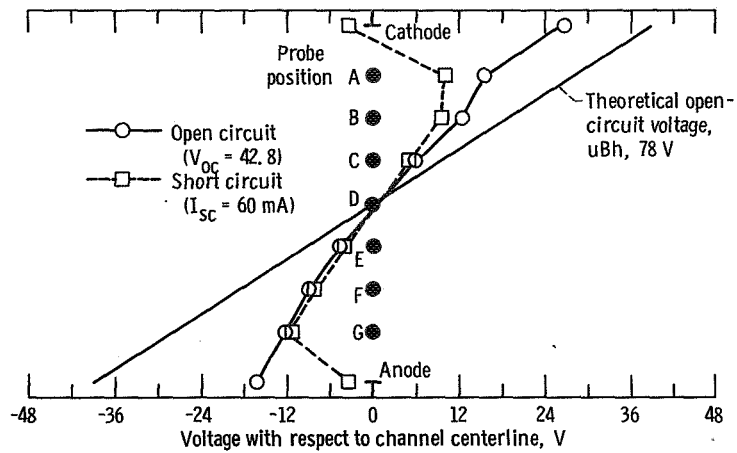


Figure 8. - Voltage profile between anode and cathode of electrode pair 1 at open- and short-circuit conditions. Magnetic-field strength, 1.46 T.

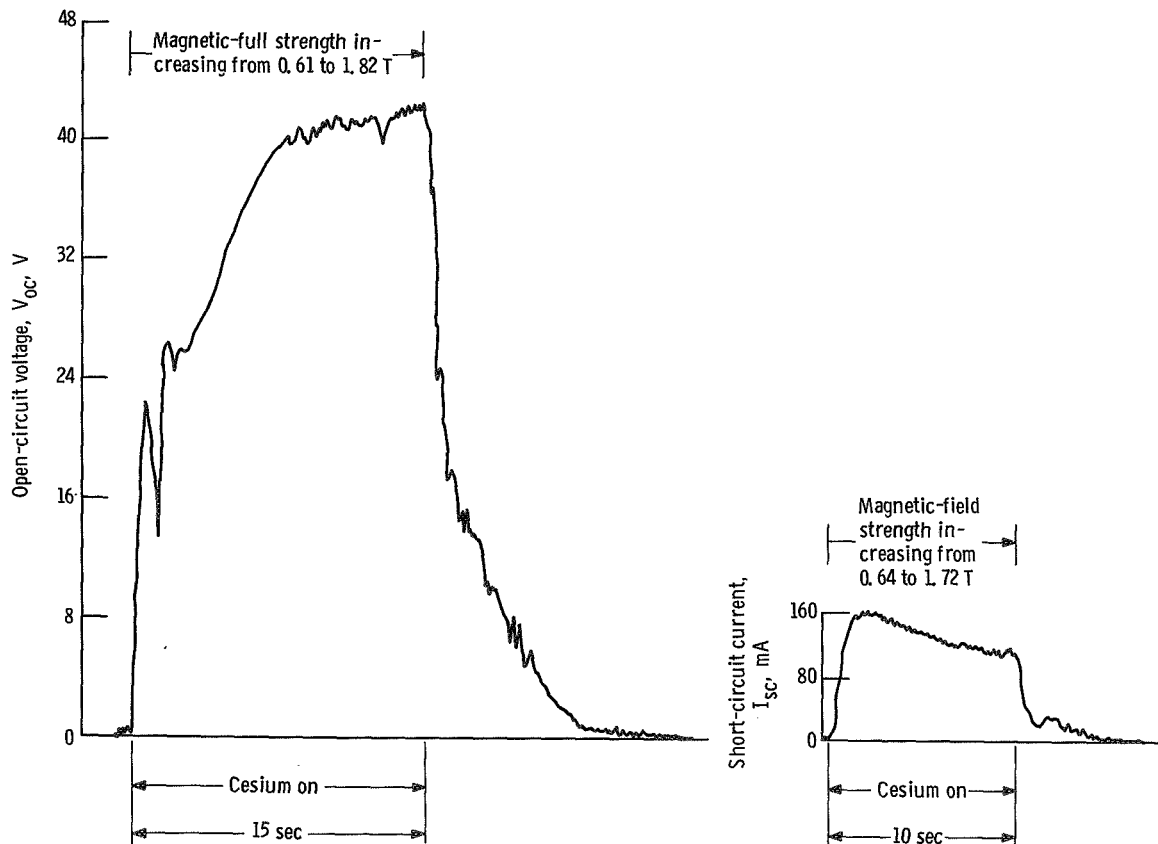


Figure 9. - Open-circuit voltage and short-circuit current during cesium injection.

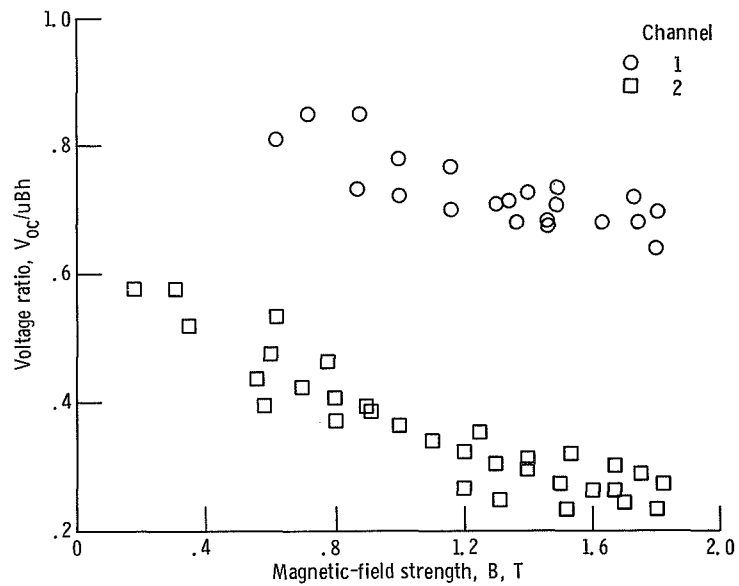


Figure 10. - Comparison of ratio of open-circuit voltage to theoretical value for two channels.

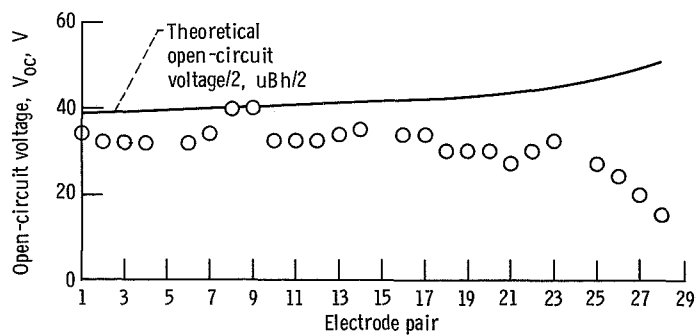


Figure 11. - Variation of open-circuit voltage along channel. Magnetic-field strength, 1.0 T.

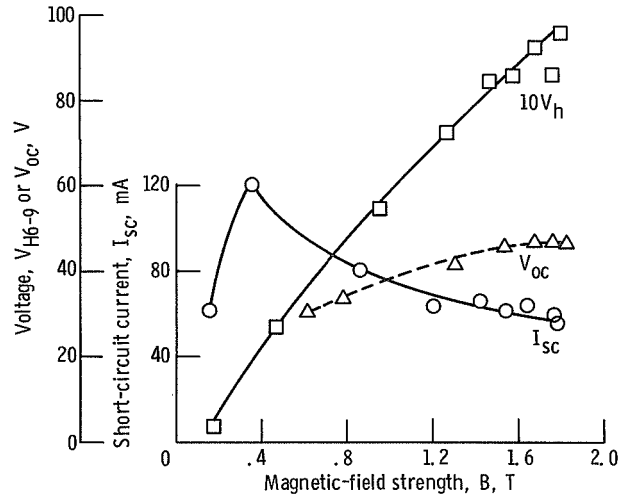


Figure 12. - Typical variation of short-circuit current and open-circuit voltage for electrode pair 7 and Hall voltage for electrode pairs 6 to 9 with magnetic-field strength.

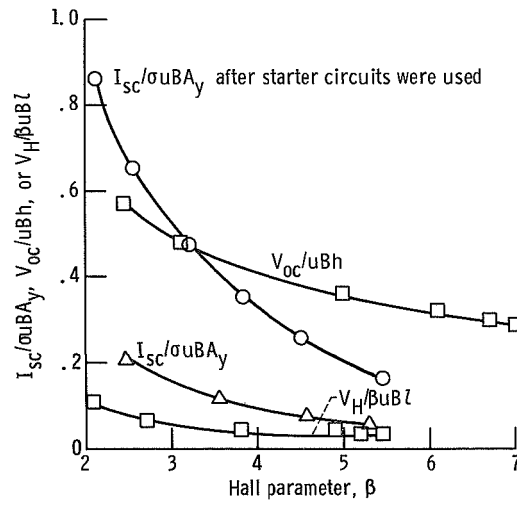


Figure 13. - Variation of $I_{sc}/\sigma uBA_y$, V_{oc}/uBh , and $V_H/\beta uBz$ with Hall parameter.

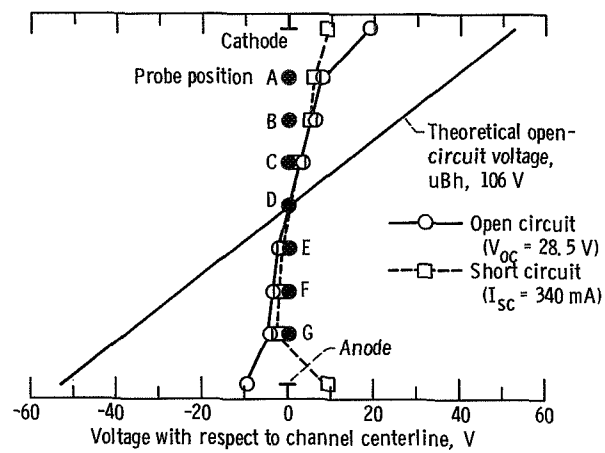


Figure 14. - Voltage profile between anode and cathode of electrode pair 1 at open- and short-circuit conditions. Magnetic-field strength, 1.18 T.

NATIONAL AERONAUTICS AND SPACE ADMINISTRATION
WASHINGTON, D. C. 20546
OFFICIAL BUSINESS
PENALTY FOR PRIVATE USE \$300

FIRST CLASS MAIL



POSTAGE AND FEES PAID
NATIONAL AERONAUTICS AND
SPACE ADMINISTRATION

POSTMASTER: If Undeliverable (Section 158
Postal Manual) Do Not Return

"The aeronautical and space activities of the United States shall be conducted so as to contribute . . . to the expansion of human knowledge of phenomena in the atmosphere and space. The Administration shall provide for the widest practicable and appropriate dissemination of information concerning its activities and the results thereof."

—NATIONAL AERONAUTICS AND SPACE ACT OF 1958

NASA SCIENTIFIC AND TECHNICAL PUBLICATIONS

TECHNICAL REPORTS: Scientific and technical information considered important, complete, and a lasting contribution to existing knowledge.

TECHNICAL NOTES: Information less broad in scope but nevertheless of importance as a contribution to existing knowledge.

TECHNICAL MEMORANDUMS: Information receiving limited distribution because of preliminary data, security classification, or other reasons.

CONTRACTOR REPORTS: Scientific and technical information generated under a NASA contract or grant and considered an important contribution to existing knowledge.

TECHNICAL TRANSLATIONS: Information published in a foreign language considered to merit NASA distribution in English.

SPECIAL PUBLICATIONS: Information derived from or of value to NASA activities. Publications include conference proceedings, monographs, data compilations, handbooks, sourcebooks, and special bibliographies.

TECHNOLOGY UTILIZATION PUBLICATIONS: Information on technology used by NASA that may be of particular interest in commercial and other non-aerospace applications. Publications include Tech Briefs, Technology Utilization Reports and Technology Surveys.

Details on the availability of these publications may be obtained from:

SCIENTIFIC AND TECHNICAL INFORMATION OFFICE

NATIONAL AERONAUTICS AND SPACE ADMINISTRATION

Washington, D.C. 20546